Int. J. Solids Structures Vol. 24, No. 3, pp. 271–284, 1988
Printed in Great Britain.

0020–7683/88 $3.00 + .00
Pergamon Press plc

OUT-OF-PLANE DYNAMIC RESPONSE OF CURVED BEAMS—AN ANALYTICAL MODEL

JÚLIO M. MONTALVÃO E SILVA and ANTÓNIO P. V. URGUEIRA†
Department of Mechanical Engineering, I.S.T., Technical University of Lisbon,
Av. Rovisco Pais, 1000 Lisboa, Portugal

(*Received* 17 *April* 1986; *in revised form* 21 *July* 1987)

Abstract—An analytical model for the vibration response of a curved beam is developed and presented. The model is based on the solution (closed solution) of the dynamic differential equations of equilibrium for an infinitesimal element vibrating out of its initial plane of curvature and allows for inclusion of the effects of rotary inertia and/or shear deformation. Final solutions are presented under the form of elements of the tip dynamic stiffness matrix for a free–free beam. The validity of the model is assessed by comparison of theoretical and experimental results for several examples of curved beams.

1. INTRODUCTION

Accurate knowledge of the vibration response of curved beams is of great importance in many engineering applications such as the design of machines and structures.

Out-of-plane vibrations of complete and incomplete rings have been the subject of interest for several research workers. In 1944 Love[1] derived the equations of out-of-plane vibrations of curved rods and presented an analytical solution for a circular ring. Den Hartog[2] applied the Rayleigh–Ritz method to compute the lowest natural frequency of circular arcs and his work was extended by Volterra and Morell[3] for the vibrations of arcs having centrelines in the form of cycloids, catenaries or parabolas. Wang[4] further extended Den Hartog's work to vibrations of elliptical arcs. Later, Culver and Oestel[5] and Wang *et al.*[6] developed an analytical technique to derive the natural frequencies of multispan circular beams.

The previous studies were based upon the classical theory in which neither the rotary inertia nor the shear deformation are taken into account. More accurate models were presented by Rao[7] and Kirkhope[8] who studied the free vibration of circular rings based on the Timoshenko theory[9]. Using the transfer matrix approach Irie *et al.*[10] determined the steady state out-of-plane response of a Timoshenko curved beam with internal damping. More recently Wang *et al.*[11] obtained the dynamic stiffness matrix for a curved beam. However, in Wang *et al.*'s work the effects of rotary inertia and shear deformation are not completely included as a consequence of neglecting the term which takes into account the effect of rotary inertia due to the rotational (torsional) vibrations which are coupled to the flexural vibrations. The purpose of the present work, is to present an analytical model where the dynamic stiffness matrix elements allow for inclusion of the full effects of rotary inertia and/or shear deformation. Theoretical results are confirmed by experimental analysis, for several examples, and are compared with results obtained using Wang *et al.*'s model[11] showing that the latter fails to provide accurate responses.

2. MATHEMATICAL FORMULATION AND SOLUTIONS

Let us consider an infinitesimal element of a curved beam with a cross-sectional shape which is assumed to remain constant along its entire length and doubly symmetric, i.e. the shear centre and centroid coincide. Due to double symmetry in-plane vibration response and torsion will be uncoupled. However, a coupling of the out-of-plane normal bending and the torsional responses will exist and will be discussed here.

Figure 1 shows an infinitesimal element of a curved member where internal forces V_y,

† Present address: Faculty of Science and Technology, New University of Lisbon, 2825 Monte da Caparica, Portugal.

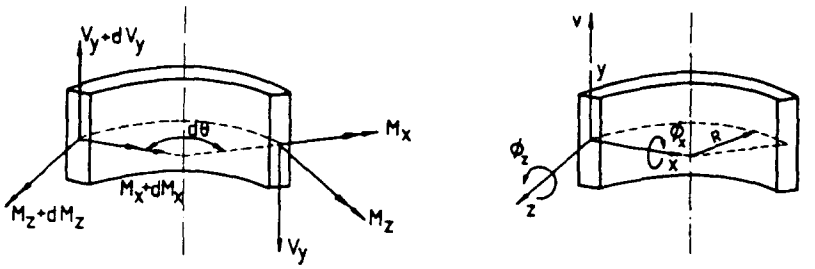

Fig. 1. Forces and displacements on a differential element of a curved beam in out-of-plane vibration.

M_x and M_z are represented as well as the related displacement v of the centreline and the rotations ϕ_x and ϕ_z of the local axes during deformation.

Rao[7], using Hamilton's principle and neglecting the warping deformation of the cross-section obtained the following dynamic equilibrium equations:

$$\frac{\partial V_y}{\partial \theta} - \rho A R \frac{\partial^2 v}{\partial t^2} = 0 \tag{1}$$

$$\frac{\partial M_x}{\partial \theta} + M_z - V_y R + \rho R I_x \frac{\partial^2 \phi_x}{\partial t^2} = 0 \tag{2}$$

$$\frac{\partial M_z}{\partial \theta} - M_x - \rho R J_z \frac{\partial^2 \phi_z}{\partial t^2} = 0. \tag{3}$$

The transverse shearing force V_y is given by

$$V_y(\theta, t) = K' G A \beta_x \tag{4}$$

where K' is a numerical factor which takes into account the variation of the shear deformation β_x through the cross-section, and is constant for any given cross-section[12]. The shear deformation is related to the slope of the transverse deflection v by

$$\frac{1}{R}\frac{\partial v}{\partial \theta} = \phi_x + \beta_x. \tag{5}$$

The moment-displacement relationships, considering the effect of shear deformation, can be expressed as

$$M_x(\theta, t) = \frac{E I_x}{R}\left(\phi_z - \frac{\partial \phi_x}{\partial \theta}\right) \tag{6}$$

$$M_z(\theta, t) = \frac{C_z}{R}\left(\phi_x + \frac{\partial \phi_z}{\partial \theta}\right). \tag{7}$$

Substituting eqns (4), (6) and (7) into the equilibrium equations, eqns (1)–(3), and noting eqn (5), one obtains[13]

$$\frac{\partial^6 v}{\partial \theta^6} + 2\frac{\partial^4 v}{\partial \theta^4} + \frac{\partial^2 v}{\partial \theta^2} - \frac{\rho R^2}{G}\left(\frac{1}{K'} + \frac{AR^2 G}{C_z}\right)\frac{\partial^2 v}{\partial t^2} - \frac{\rho^2 R^4}{G^2}\left(\frac{I_x G}{K' C_z} + \frac{G J_z}{K' E I_x}\right.$$
$$\left. + \frac{AR^2 G^2 J_z}{C_z E I_x}\right)\frac{\partial^4 v}{\partial t^4} - \frac{\rho^3 R^6 J_z}{G E K' C_z}\frac{\partial^6 v}{\partial t^6} + \frac{\rho R^2}{G}\left(\frac{AR^2 G}{E I_x} - \frac{2}{K'} + \frac{I_x G}{C_z} + \frac{G J_z}{E I_x}\right)\frac{\partial^4 v}{\partial \theta^2 \partial t^2}$$
$$- \frac{\rho R^2}{G}\left(\frac{J_z G}{C_z} + \frac{1}{K'} + \frac{G}{E}\right)\frac{\partial^6 v}{\partial \theta^4 \partial t^2} + \frac{\rho^2 R^4}{G^2}\left(\frac{J_z G}{K' C_z} + \frac{G^2 J_z}{E C_z} + \frac{G}{K' E}\right)\frac{\partial^6 v}{\partial \theta^2 \partial t^4} = 0 \tag{8}$$

$$\left(1+\frac{C_z}{K'GAR}\right)\phi_x+\frac{\rho I_x}{K'GA}\frac{\partial^2\phi_x}{\partial t^2}=-\frac{\rho EI_x}{K'^2G^2AR}\frac{\partial^3 v}{\partial\theta\,\partial t^2}$$
$$+\frac{EI_x}{K'GAR}\frac{\partial^3 v}{\partial\theta^3}+\frac{1}{R}\frac{\partial v}{\partial\theta}-\left(\frac{EI_x+C_z}{K'GAR^2}\right)\frac{\partial\phi_z}{\partial\theta} \quad (9)$$

$$R\phi_z+\frac{\rho J_z R^3}{EI_x}\frac{\partial^2\phi_z}{\partial t^2}=\frac{C_z+EI_x}{EI_x}\left(\frac{\partial^2 v}{\partial\theta^2}-\frac{\rho R^2}{K'G}\frac{\partial^2 v}{\partial t^2}\right)$$
$$+\frac{C_z}{EI_x}\frac{1}{EI_x+C_z}\left\{EI_x\frac{\partial^4 v}{\partial\theta^4}-C_z\frac{\partial^2 v}{\partial\theta^2}-\rho I_x R^2\left(\frac{E}{K'G}+1\right)\frac{\partial^4 v}{\partial\theta^2\,\partial t^2}\right.$$
$$\left.-\rho R^2\left(AR^2+\frac{C_z}{K'G}\right)\frac{\partial^2 v}{\partial t^2}+\frac{\rho^2 I_x R^4}{K'G}\frac{\partial^4 v}{\partial t^4}\right\}. \quad (10)$$

Assuming now that the curved member is excited harmonically, with a frequency ω, we have

$$v(\theta,t)=V(\theta)\,e^{i\omega t} \quad (11a)$$
$$\phi_x(\theta,t)=\Phi_x(\theta)\,e^{i\omega t} \quad (11b)$$
$$\phi_z(\theta,t)=\Phi_z(\theta)\,e^{i\omega t} \quad (11c)$$

and

$$V_y(\theta,t)=\tilde{V}_y(\theta)\,e^{i\omega t} \quad (12a)$$
$$M_x(\theta,t)=\tilde{M}_x(\theta)\,e^{i\omega t} \quad (12b)$$
$$M_z(\theta,t)=\tilde{M}_z(\theta)\,e^{i\omega t} \quad (12c)$$

Substituting eqns (11) into eqns (8)–(10) and noting that the value of $\partial\phi_z/\partial\theta$ obtained from the resulting eqn (10) was introduced in the resulting eqn (9), one obtains

$$\frac{d^6V(\theta)}{d\theta^6}+A_4\frac{d^4V(\theta)}{d\theta^4}+A_2\frac{d^2V(\theta)}{d\theta^2}+A_0V(\theta)=0 \quad (13)$$

$$R\Phi_x(\theta)=C_6\left\{C_5\frac{d^5V(\theta)}{d\theta^5}+C_3\frac{d^3V(\theta)}{d\theta^3}+C_1\frac{dV(\theta)}{d\theta}\right\} \quad (14)$$

$$R\Phi_z(\theta)=B_5\left\{\frac{d^4V(\theta)}{d\theta^4}+B_2\frac{d^2V(\theta)}{d\theta^2}+B_0V(\theta)\right\} \quad (15)$$

where the values of the coefficients A_4, A_2, A_0, C_6, C_5, C_3, C_1, B_5, B_2 and B_6 are given by the expressions presented in Appendix A.

It can be seen that $\Phi_x(\theta)$ and $\Phi_z(\theta)$ are functions of $V(\theta)$ only, which in turn is a solution of the linear differential equation, eqn (13), and can be rewritten as

$$V(\theta)=[D(\theta)]\{X\}. \quad (16)$$

The expressions for the elements of the row matrix $[D(\theta)]$ are given in Appendix B, for the different roots of the auxiliary equation the solutions of which are also presented in

Appendix B. The elements of vector $\{X\}$ are the six constants X_i that can be determined from knowledge of the boundary conditions.

Thus the displacements of the centreline for a given value θ can be expressed as

$$\{\delta\}_\theta = \begin{Bmatrix} V(\theta) \\ R\Phi_x(\theta) \\ R\Phi_z(\theta) \end{Bmatrix} = [A(\theta)]\{X\} \tag{17}$$

where matrix $[A(\theta)]$ is given by

$$[A(\theta)] = \begin{bmatrix} [D(\theta)] \\ C_6[C_5[D^{(v)}(\theta)] + C_3[D'''(\theta)] + C_1[D'(\theta)]] \\ B_5[[D^{(iv)}(\theta)] + B_2[D''(\theta)] + B_0[D(\theta)]] \end{bmatrix} \tag{18}$$

where the primes represent differentiations with respect to θ.

Substituting eqns (11) and (12) into eqns (4), (6) and (7) and omitting the common term $e^{i\omega t}$ yields

$$\{P\} = \begin{Bmatrix} \tilde{V}_y(\theta) \\ \tilde{M}_x(\theta)/R \\ \tilde{M}_z(\theta)/R \end{Bmatrix} = \frac{EI_x}{R^3}[B(\theta)]\{X\} \tag{19}$$

matrix $[B(\theta)]$ being given by

$$[B(\theta)] = \begin{bmatrix} V_{y5}[D^{(v)}(\theta)] + V_{y3}[D'''(\theta)] + V_{y1}[D'(\theta)] \\ M_{x6}[D^{(vi)}(\theta)] + M_{x4}[D^{(iv)}(\theta)] + M_{x2}[D''(\theta)] + M_{x0}[D(\theta)] \\ M_{z5}[D^{(v)}(\theta)] + M_{z3}[D'''(\theta)] + M_{z1}[D'(\theta)] \end{bmatrix} \tag{20}$$

where V_{yi}, M_{xi} and M_{zi} are coefficients given by the expressions presented in Appendix A.

3. DYNAMIC STIFFNESS MATRIX

The generalized displacements and forces associated with the tips of the analytical model of our curved beam are shown in Fig. 2. Vector $\{\delta\}$ representing the generalized displacements at each end of the curved member can be written as

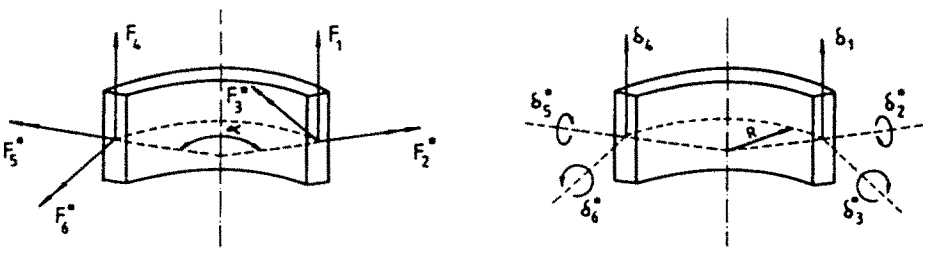

Fig. 2. Positive generalized forces and displacements associated with the model of a curved beam (note that F_1^*, F_2^*, F_3^* and F_6^* represent F_1R, F_2R, F_3R and F_6R, respectively, and δ_1^*, δ_2^*, δ_3^* and δ_6^* are equal to δ_1/R, δ_2/R, δ_3/R and δ_6/R, respectively).

$$\{\delta\} = \begin{Bmatrix} V(0) \\ R\Phi_x(0) \\ R\Phi_z(0) \\ \hline V(\alpha) \\ R\Phi_x(\alpha) \\ R\Phi_z(\alpha) \end{Bmatrix} = [A_t]\{X\} \tag{21}$$

with matrix $[A_t]$ given by

$$[A_t] = \begin{bmatrix} A(0) \\ \hline A(\alpha) \end{bmatrix}.$$

Similarly, vector $\{F\}$ representing the generalized forces at the tip of the curved member can be written as

$$\{F\} = \begin{Bmatrix} F_1 \\ F_2 \\ F_3 \\ F_4 \\ F_5 \\ F_6 \end{Bmatrix} = [Q] \begin{Bmatrix} \tilde{V}_y(0) \\ \tilde{M}_x(0)/R \\ \tilde{M}_z(0)/R \\ \hline \tilde{V}_y(\alpha) \\ \tilde{M}_x(\alpha)/R \\ \tilde{M}_z(\alpha)/R \end{Bmatrix} = \frac{EI_x}{R^3}[Q][B_t]\{X\} \tag{22}$$

with transformation matrix $[Q]$ and matrix $[B_t]$ given by

$$[Q] = \begin{bmatrix} -1 & 0 & 0 & 0 & 0 & 0 \\ 0 & 1 & 0 & 0 & 0 & 0 \\ 0 & 0 & -1 & 0 & 0 & 0 \\ 0 & 0 & 0 & 1 & 0 & 0 \\ 0 & 0 & 0 & 0 & -1 & 0 \\ 0 & 0 & 0 & 0 & 0 & 1 \end{bmatrix}$$

and

$$[B_t] = \begin{bmatrix} B(0) \\ \hline B(\alpha) \end{bmatrix}.$$

Using eqn (21) vector $\{X\}$ can be related with vector $\{\delta\}$ through the expression

$$\{X\} = [A_t]^{-1}\{\delta\}. \tag{23}$$

Substituting into eqn (22) one obtains

$$\{F\} = [K_d]\{\delta\} \tag{24}$$

where matrix $[K_d]$ is the so-called dynamic stiffness matrix, and is given by

$$[K_d] = \frac{EI_x}{R^3}[Q][B_t][A_t]^{-1}. \tag{25}$$

4. INCLUSION OF STRUCTURAL DAMPING EFFECTS

The derivation of the expressions previously presented was carried out making no reference to the energy dissipation effects. However, structural damping must be accounted for if one intends to obtain accurate results particularly near to the resonance frequencies. Inclusion of the effects of structural damping in the dynamic stiffness expressions is an easy task and can be done considering the complex representation of E and G[14]

$$E^* = E(1+i\eta_E)$$
$$G^* = G(1+i\eta_G)$$

where η_E and η_G represent the loss factor associated with E and G, respectively. For our purpose η_E and η_G can be considered as having the same value and being frequency independent. Hence the elements of vector $\{F\}$ and $\{\delta\}$ and of matrices $[A_i]$ and $[B_i]$ are complex quantities, for the damped model, and can be obtained from the corresponding elements in the real matrices derived for the undamped model, simply by replacing E and G by their corresponding complex representations E^* and G^*.

5. PRESENTATION OF RESULTS

In order to assess the validity of the derived theoretical model, it was decided to test several curved beams with different cross-sections and different radii of curvature as shown in Fig. 3. The frequency range of the experimental analysis was chosen to cover the first four or five resonance frequencies of the test beams. Accuracy was of great concern and therefore the test procedure was based on a step-by-step harmonic excitation using a Transfer Function Analyser, thus measuring the acceleration response/force excitation relationship for each exciting frequency throughout the test range. Acceleration and force were measured using small piezoelectric transducers together with signal conditioning amplifiers and the excitation was provided by means of an electromagnetic shaker driven by the Transfer Function Analyser through an adequate power amplifier. Calibration of the transducers was carefully verified[14] prior to the experimental analysis. The exciting force was applied in a direction normal to the plane of curvature of the beam and the acceleration response was measured in the same direction, the measurement points being chosen at the tips of the test beam. Experimental results are presented in terms of the $\ddot{\delta}/F$ relationship (inertance).

Figure 4 is presented as an example of the results obtained. The curves displayed allow for comparison of the direct inertance $\ddot{\delta}/F$ measured at the tip of a curved beam with the theoretically derived responses using the model presented in this work and classical theory. An extra theoretical curve according to Wang *et al.*'s model[11], is also presented.

Similar results were obtained for all the other measured response curves and for all the test beams. They are not presented here in order not to extend too much the size of this paper. Table 1 summarizes the results in terms of the values of the resonance frequencies, taken from the response curves, for different curved beams. The results obtained from the model presented in this paper are clearly better than the ones obtained with classical theory or with Wang *et al.*'s model, when compared with experimental data. There are still some discrepancies between the theoretical and test results, the latter presenting consistently lower values for the resonance frequencies. It is believed that this is mainly due to the test conditions where, for example, the additional mass of the transducers contributes to lower the experimental resonance frequencies.

Table 2 shows the influence in the results when rotary inertia and shear deformation are included in the model. For example, it is clearly seen that the effects of rotary inertia are mainly felt below 90°.

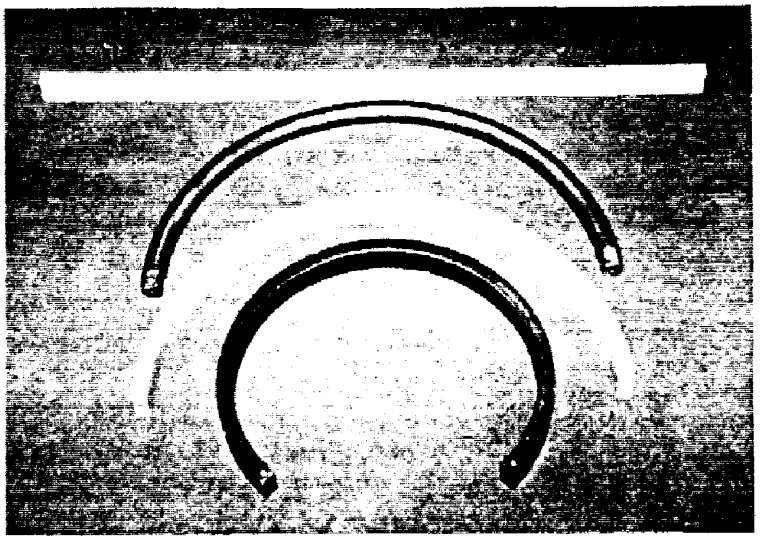

Fig. 3. Test beams.

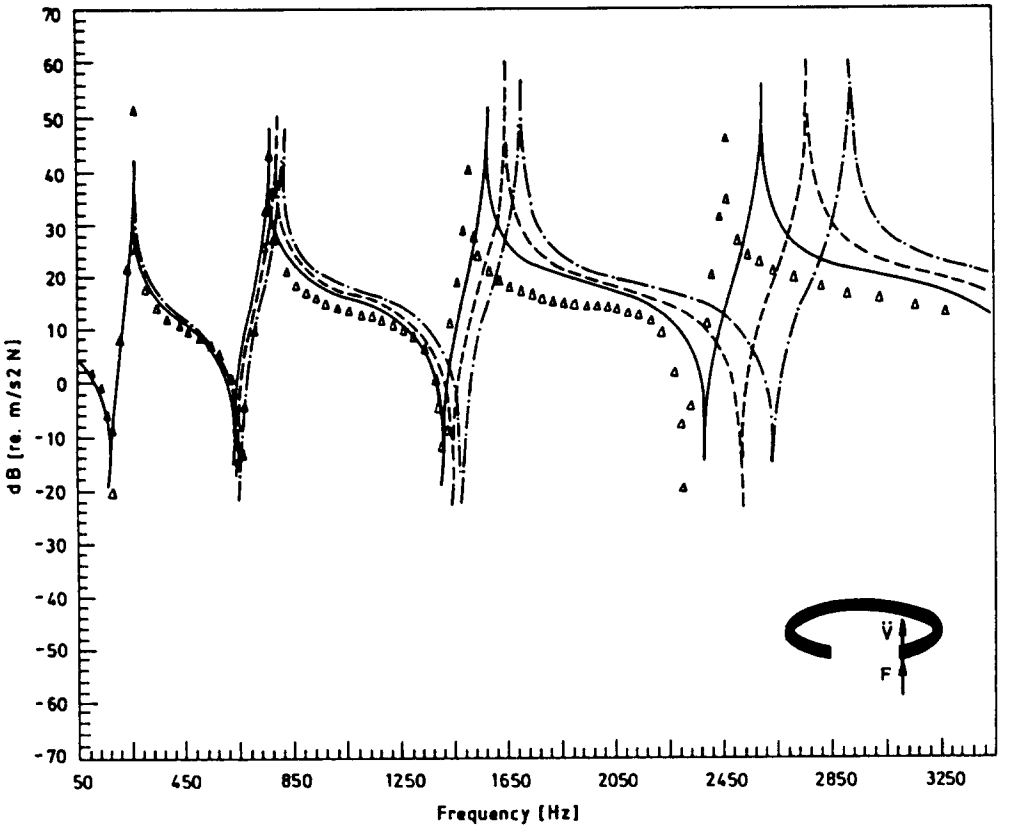

Fig. 4. Direct inertance at the tip of a curved beam ($\nu = 0.288$, $K' = 0.849$, $\rho = 7755$ kg m^{-3}, $E = 209$ GPa, $I_z = 4.369 \times 10^{-8}$ m^4, $R/h = 10$, $R = 0.16$ m, $\alpha = 270°$): △△△, experimental values; ——, present model; - - - - -, Wang *et al.*'s model[11]; — · — · —, classical theory.

For the same beams, with different radii of curvature, the variation of the values of the resonance frequencies with the corresponding angle α is presented in Fig. 5. It can be seen that the resonance frequencies tend to those obtained for a straight beam when the radius of curvature is large. This fact further validates the theoretical discussion.

Table 1. Resonance frequencies for different curved beams; (A) classical theory; (B) Wang *et al.*'s model[11]; (C) present model

		R_1	R_2	R_3	R_4
30°	A	796.75	1466.1	2642.5	3458.5
	B	782.87	1418.6	2494.2	3675.0
	C	632.36	779.6	1570.7	2153.4
60°	A	727.2	1421.2	2562.5	3550.6
	B	715.46	1376.0	2424.8	3459.3
	C	707.29	1046.4	1671.2	2167.4
90°	A	639.18	1351.8	2456.0	3614.2
	B	630.2	1310.7	2328.8	3451.3
	C	620.25	1190.2	2022.2	2136.2
180°	A	400.3	1067.2	2074.1	3370.4
	B	400.2	1047.8	1992.5	3143.4
	C	391.05	1007.2	1882.2	2818.0
	Exp.	387.5	967.6	1717.5	2763.0
270°	A	254.2	792.9	1690.5	2910.3
	B	255.0	784.1	1638.2	2752.0
	C	250.8	760.4	1564.2	2580.0
	Exp.	250.5	747.1	1487.5	2460.2

Note: The length of the different beams has the same value 0.754 m, and the same cross-section dimensions 0.016 × 0.032 m.

Table 2. Comparison of values of resonance frequencies obtained using different models; (A) classical theory—rotary inertia and shear deformation neglected; (B) rotary inertia included and shear deformation neglected; (C) present model—rotary inertia and shear deformation included

		R_1	R_2	R_3	R_4
30°	A	796.75	1466.1	2642.5	3458.5
	B	634.21	786.33	1605.1	2162.4
	C	632.36	779.6	1570.7	2153.4
60°	A	727.2	1421.2	2562.5	3550.6
	B	712.36	1053.5	1700.8	2197.8
	C	707.29	1046.4	1671.2	2167.4
90°	A	639.18	1351.8	2456.0	3614.2
	B	623.42	1203.4	2045.6	2180.2
	C	620.25	1190.2	2022.2	2136.2
180°	A	400.3	1067.2	2074.1	3370.4
	B	395.81	1023.4	1927.9	2864.3
	C	391.05	1007.2	1882.2	2818.0
270°	A	254.2	792.9	1690.5	2910.3
	B	253.7	771.19	1596.9	2657.8
	C	250.8	760.4	1564.2	2580.0

Finally, Fig. 6 is another example presenting the response curves for the particular case where the angle α is 60°, and shows clearly that Wang *et al.*'s model[11] fails to predict accurate and complete responses. As stated previously these inaccuracies are due to neglecting the rotary inertia associated with the coupled torsional behaviour of the curved beam.

6. CONCLUSIONS

An analytical model for the out-of-plane vibration response of curved beams was derived. The coupling of bending and torsion responses was taken into account and the

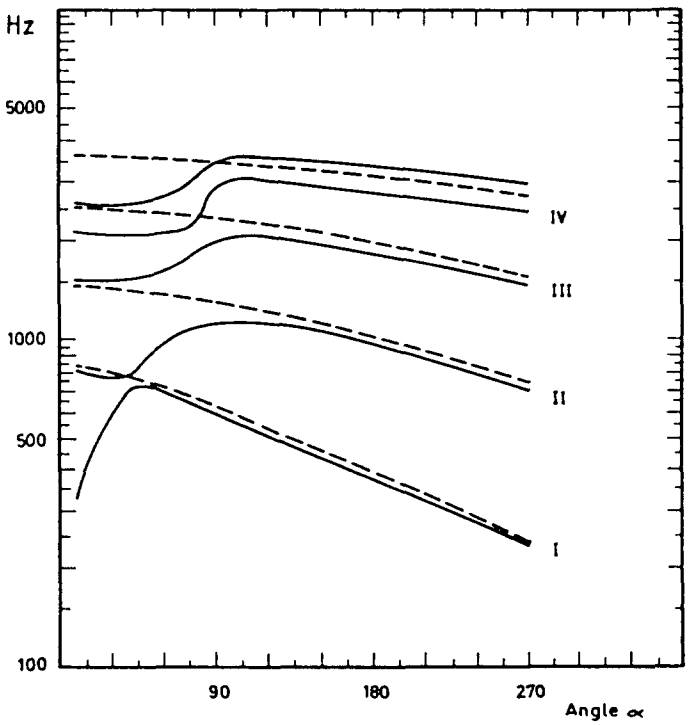

Fig. 5. Variation of the resonance frequencies with corresponding angle α: ——, present model; ------, Wang *et al.*'s model[11].

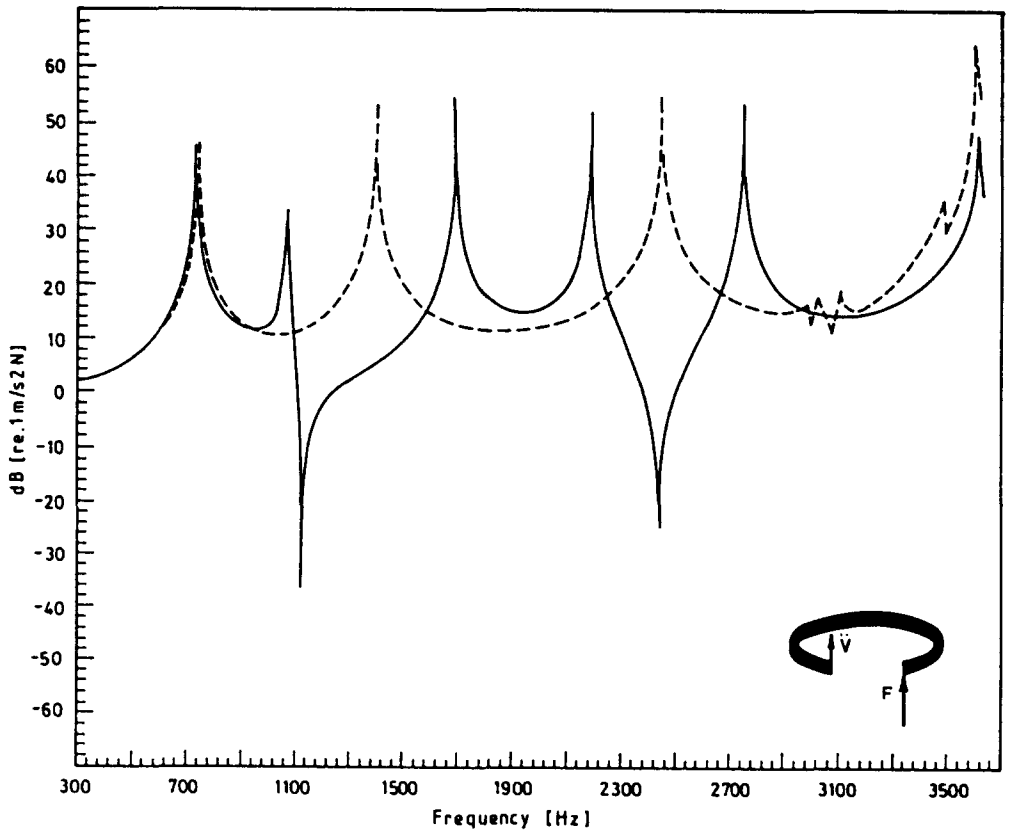

Fig. 6. Example of transferred inertance obtained for the particular case where the angle α is 60°: ——, present model; - - - - -, Wang *et al.*'s model[11].

model allowed for inclusion of the full effects of rotary inertia and shear deformation as well as structural damping. The final theoretical expressions were presented in terms of the elements of the tip dynamic stiffness matrix. It was shown that the rotary inertia associated with coupling with torsional effects cannot be neglected, by comparison of results with those obtained using such a model. The validity of the analytical model was confirmed by means of experimental analysis.

Acknowledgement—The financial support of the Portuguese National Institute of Scientific Research (INIC) awarded to the Centre of Mechanics and Materials of the Technical University of Lisbon (CEMUL) where the authors conducted this investigation is gratefully acknowledged.

REFERENCES

1. A. E. H. Love, *A Treatise on the Mathematical Theory of Elasticity*, 4th Edn. Dover, New York (1944).
2. J. P. Den Hartog, *Mechanical Vibrations*, 4th Edn. McGraw-Hill, New York (1956).
3. E. Volterra and J. D. Morell, Lowest natural frequency of elastic arc for vibrations outside the plane of initial curvature. *J. Appl. Mech.* **28**, 624–627 (1961).
4. T. M. Wang, Fundamental frequency of campled elliptic arcs for vibrations outside the plane of initial curvature. *J. Sound Vibr.* **42**, 515–519 (1975).
5. C. G. Culver and D. J. Oestel, Natural frequencies of multispan curved beams. *J. Sound Vibr.* **10**, 380–389 (1969).
6. T. M. Wang, R. H. Nettleton and B. Keita, Natural frequencies for out-of-plane vibrations of continuous curved beams. *J. Sound Vibr.* **68**, 427–436 (1980).
7. S. S. Rao, Effects of transverse shear and rotary inertia on the coupled twist-bending vibrations of circular rings. *J. Sound Vibr.* **16**, 551–566 (1971).
8. J. Kirkhope, Out-of-plane vibration of thick circular ring. *J. Engng Mech. Div.* **102**(EM2), 239–247 (1976).
9. S. P. Timoshenko, D. H. Young and W. Weaver, *Vibration Problems in Engineering*, 4th Edn. Wiley, New York (1974).
10. T. Irie, G. Yamada and I. Takahashi, The steady state out-of-plane response of a Timoshenko curved beam with internal damping. *J. Sound Vibr.* **71**, 145–156 (1980).
11. T. M. Wang, A. Laskey and M. Ahmad, Natural frequencies for out-of-plane vibrations of continuous curved beams considering shear and rotary inertia. *Int. J. Solids Structures* **20**, 257–265 (1984).
12. G. R. Cowper, The shear coefficient in Timoshenko's beam theory. *J. Appl. Mech.* **33**, 335–340 (1966).

13. A. P. V. Urgueira, Dynamic analysis of curved beams–development of an analytical model. M.Sc. Thesis (in Portuguese), I.S.T., Technical University of Lisbon (1985).
14. J. M. M. Silva, Measurements and applications of structural mobility data for the vibration analysis of complex structures. Ph.D. Thesis, Imperial College, London (1978).

APPENDIX A

Coefficients of eqn (13)

$$A_4 = 2+qr\left(1+\frac{1}{ab}\right)+qs$$

$$A_2 = 1-q+2qs-qr\left(\frac{a+b}{ab}\right)+q^2rs\left(1+\frac{1}{ab}\right)+\frac{q^2r^2}{ab}$$

$$A_0 = \frac{q}{a}+qs-q^2rs\left(\frac{a+b}{ab}\right)-\frac{q^2r}{ab}+q^3r^2s\frac{1}{ab}$$

with

$$q = \frac{\rho AR^4\omega^2}{EI_x} \quad \text{(bending effect)}$$

$$r = \frac{I_x}{AR^2} \quad \text{(rotary inertia effect)}$$

$$s = \frac{EI_x}{K'GAR^2} \quad \text{(shear deformation effect)}$$

$$a = \frac{C_z}{EI_x}$$

where $C_z = \chi GJ_z$, with χ a constant depending on the cross-section form

$$b = \frac{I_x}{J_z}.$$

Coefficients of eqn (14)

$$C_6 = a/[(qrs-as-1)(1-qr/b)]$$

$$C_5 = s$$

$$C_3 = 2s+qrs\left(1+\frac{1}{ab}\right)+qs^2$$

$$C_1 = 2qs^2-qs-1/a+q^2rs^2\left(1+\frac{1}{ab}\right)+\frac{qr}{ab}.$$

Coefficients of eqn (15)

$$B_5 = a/[(1-qr/b)(1+a)]$$

$$B_2 = \frac{1+2a}{a}+qr+qs$$

$$B_0 = -q+q^2rs+qs\left(\frac{1+2a}{a}\right).$$

Coefficients in matrix $[B(0)]$—expression (20)

$$V_{r3} = -C_6$$

$$V_{r3} = -C_6C'_3$$

$$V_{r1} = C_6C'_1$$

with coefficients C'_3 and C'_1 given by

$$C'_3 = 2+qr\left(1+\frac{1}{ab}\right)+qs$$

$$C'_1 = q-1+qr\left(\frac{a+b}{ab}\right)-2qs-\frac{q^2r^2}{ab}-q^2rs\left(1+\frac{1}{ab}\right)$$

$$M_{x6} = -C_6C_5$$
$$M_{x4} = B_5-C_6C_3$$
$$M_{x2} = B_5B_2-C_6C_1$$
$$M_{x0} = B_5B_0$$
$$M_{z5} = a(C_6C_5+B_5)$$
$$M_{z3} = a(C_6C_3+B_5B_2)$$
$$M_{z1} = a(C_6C_1+B_5B_0).$$

APPENDIX B

The characteristic equation associated with eqn (13) is given by

$$\lambda^6+A_4\lambda^4+A_2\lambda^2+A_0 = 0. \tag{B1}$$

In order to obtain the Cardan form we can assume $\lambda^2 = \gamma-A_4/3$ and then

$$\gamma^3+\Pi\gamma+\Gamma = 0 \tag{B2}$$

with

$$\Pi = A_2-A_4^2/3$$
$$\Gamma = \frac{2}{27}A_4^3-\frac{1}{3}A_4A_2+A_0.$$

The discriminant of this polynomial is given by

$$\Delta = \frac{\Gamma^2}{4}+\frac{\Pi^3}{27}.$$

The roots of eqn (B2) depend upon the sign of Δ. Three cases are possible:

(a) $\Delta < 0$, three real and unequal roots;
(b) $\Delta = 0$, three real roots of which at least two roots are equal;
(c) $\Delta > 0$, one real root and two complex conjugate roots.

The solution of eqn (13) can be expressed as

$$V(\theta) = [D(\theta)]\{X\}.$$

Hence, matrix $[D(\theta)]$ can assume three different forms.

Case (1): $\Delta < 0$, i.e. three negative roots, γ_1, γ_2 and γ_3

$$[D(\theta)] = [\cos(\lambda_1\theta)\ \cos(\lambda_2\theta)\ \cos(\lambda_3\theta)\ \sin(\lambda_1\theta)\ \sin(\lambda_2\theta)\ \sin(\lambda_3\theta)].$$

Case (2): $\Delta < 0$, i.e. one negative root γ_1

$$[D(\theta)] = [\cos(\lambda_1\theta)\ \cosh(\lambda_2\theta)\ \cosh(\lambda_3\theta)\ \sin(\lambda_1\theta)\ \sinh(\lambda_2\theta)\ \sinh(\lambda_3\theta)].$$

Case (3): $\Delta > 0$, i.e. one negative root γ_1 and two complex conjugate roots

$$[D(\theta)] = \begin{bmatrix} \cos(\lambda_1\theta) & \cos(\mu\theta)\cosh(\nu\theta) & \cos(\mu\theta)\sinh(\nu\theta) \\ \sin(\lambda_1\theta) & \sin(\mu\theta)\sinh(\nu\theta) & \sin(\mu\theta)\cosh(\nu\theta) \end{bmatrix}$$

where λ is related to γ as shown previously and ν and μ are the real and imaginary parts, respectively, of the complex roots.

APPENDIX C: NOTATION

x, y, z	curvilinear coordinates along centroidal axes
$v(\theta, t)$	displacement of the centreline along the y-axis
$V(\theta)$	modulus of v

$\phi_x(\theta, t), \phi_z(\theta, t)$ angular rotations along x and z, respectively
$\Phi_x(\theta), \Phi_z(\theta)$ moduli of ϕ_x and ϕ_z, respectively
V_y shear force along the y-axis
$\tilde{V}_y(\theta)$ modulus of V_y
M_x moment about the x-axis
M_z torque about the z-axis
$\tilde{M}_x(\theta), \tilde{M}_z(\theta)$ moduli of M_x and M_z, respectively
C_z torsional stiffness
J_z polar moment of area about the z-axis
I_x second moment of area about the x-axis
E Young's modulus
G shear modulus
ρ mass density
R radius of curvature
A area of the cross-section
i $\sqrt{-1}$
ω frequency
t time.